

UNCLASSIFIED

AD 414810

DEFENSE DOCUMENTATION CENTER

FOR

SCIENTIFIC AND TECHNICAL INFORMATION

CAMERON STATION, ALEXANDRIA, VIRGINIA



UNCLASSIFIED

NOTICE: When government or other drawings, specifications or other data are used for any purpose other than in connection with a definitely related government procurement operation, the U. S. Government thereby incurs no responsibility, nor any obligation whatsoever; and the fact that the Government may have formulated, furnished, or in any way supplied the said drawings, specifications, or other data is not to be regarded by implication or otherwise as in any manner licensing the holder or any other person or corporation, or conveying any rights or permission to manufacture, use or sell any patented invention that may in any way be related thereto.

When U.S. Government drawings, specifications, or other data are used for any purpose other than a definitely related government procurement operation, the government thereby incurs no responsibility nor any obligation whatsoever; and the fact that the government may have formulated, furnished, or in any way supplied the said drawings, specifications, or other data is not to be regarded by implication or otherwise, as in any manner licensing the holder or any other person or corporation, or conveying any rights or permission to manufacture, use, or sell any patented invention that may in any way be related thereto.

Qualified requesters may obtain copies from DDC. Orders will be expedited if placed through the librarian or other person designated to request documents from DDC.

Do not return this copy. Retain or destroy.

ABSTRACT

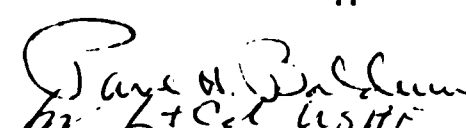
This report is the first on Contract AF30(602)-2930 and describes the experimental test program for determining the properties of the Two-dimensional Self-focusing Array Antenna Model constructed under contract AF30(602)-2297.

The initial efforts of the program have been devoted to the design and construction of the test equipment to be used in the field probing operation. The results of these efforts are described in this report. In addition, a brief discussion of the salient features of the self-focusing technique in a two-dimensional mode of operation is reviewed as background. Preliminary efforts have been made to provide more specific definitions and objectives of the tests to be performed. This is also discussed in the report.

PUBLICATION REVIEW

This report has been reviewed and is approved.

Approved:


ARTHUR J. FROHLICH
Chief, Techniques Laboratory
Directorate of Aerospace Surveillance & Control

Approved:

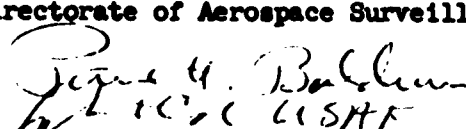

WILLIAM T. POPE
Acting Director
Director of Aerospace
Surveillance & Control

TABLE OF CONTENTS

	Page
1. INTRODUCTION AND SUMMARY	1
1.1 <u>Background</u>	1
2. DESCRIPTION OF TWO-DIMENSIONAL ARRAY	7
2.1 <u>Specifications</u>	7
2.2 <u>Construction Features</u>	7
2.3 <u>Field Measurement System</u>	18
2.4 <u>Illumination Monitor</u>	24
3. TEST PROGRAM	30
3.1 <u>Outline of Tests</u>	30
3.2 <u>Program For Next Period</u>	37
4. APPENDIX - SCATTERING OF CONVERGENT WAVES	38
1. <u>Introduction</u>	38
2. <u>The Forms of Scattering</u>	40
3. <u>Source</u>	42
4. <u>Scatterers</u>	43
5. <u>Conclusions</u>	45

LIST OF ILLUSTRATIONS

	<u>Page</u>
Figure 1 - Principle of Self-Focusing Array Antenna for Stationary or Slowly Moving Target	3
Figure 2 - Heterodyne Method for Obtaining the Phase Conjugate	5
Figure 3 - Rear View of 2-D Array	8
Figure 4 - Block Diagram of One Module	10
Figure 5 - Patterns of $2\lambda \times 2\lambda$ Horn Antenna	12
Figure 6 - Patterns of $6\lambda \times 8\lambda$ Horn Antenna	13
Figure 7 - Block Diagram of Signal Generating System	16
Figure 8 - Test Probe Assembly	21
Figure 9 - Block Diagram of Illumination Monitor	26
Figure 10 - Illumination Function Display	28
Figure 11 - Shadow Regions in 2-D Array Testing	33

1. INTRODUCTION AND SUMMARY

This first report on the investigation of the properties of a two-dimensional array model under Contract AF30(602)-2930 will describe the design and construction of the test equipment necessary for the radiation-field probing. The test program which ECI proposes to conduct has also been partially determined during the period and is discussed in later sections. An appendix which covers some initial thoughts concerning the philosophy behind the backscattering tests has been included at the end of the report. As a means of relating the two-dimensional array contract to the work done previously on a Linear Focusing Array Model, a brief review of the self-focusing technique and the reasoning behind the conversion to a two-dimensional configuration are presented.

1.1 Background

Convergent focusing is a property of the Fresnel region which extends from a distance of approximately $5D$ from the antenna to a distance of D^2/λ where D is the antenna diameter. Within this region an antenna pattern may be obtained which is the same as the Fraunhofer or far field pattern. An antenna is brought to focus at some distance, R_f , by introducing a spherical phase distribution across the antenna aperture in an array type of antenna. Three other properties of focused antennas are:

- (1) The diameter, Δ , of the circle in the focal plane defined by the half power beamwidth is

$$\Delta = 0.98 R_f \frac{\lambda}{D}$$

- (2) The distance between the first nulls of the radiation pattern at the focal plane is $\Delta_o = 2.44 R_f \lambda/D$

1. INTRODUCTION AND SUMMARY

This first report on the investigation of the properties of a two-dimensional array model under Contract AF30(602)-2930 will describe the design and construction of the test equipment necessary for the radiation-field probing. The test program which ECI proposes to conduct has also been partially determined during the period and is discussed in later sections. An appendix which covers some initial thoughts concerning the philosophy behind the backscattering tests has been included at the end of the report. As a means of relating the two-dimensional array contract to the work done previously on a Linear Focusing Array Model, a brief review of the self-focusing technique and the reasoning behind the conversion to a two-dimensional configuration are presented.

1.1 Background

Convergent focusing is a property of the Fresnel region which extends from a distance of approximately $5D$ from the antenna to a distance of D^2/λ where D is the antenna diameter. Within this region an antenna pattern may be obtained which is the same as the Fraunhofer or far field pattern. An antenna is brought to focus at some distance, R_f , by introducing a spherical phase distribution across the antenna aperture in an array type of antenna. Three other properties of focused antennas are:

- (1) The diameter, Δ , of the circle in the focal plane defined by the half power beamwidth is

$$\Delta = 0.98 R_f \frac{\lambda}{D}$$

- (2) The distance between the first nulls of the radiation pattern at the focal plane is $\Delta_o = 2.44 R_f \lambda/D$

- (3) The percentage of the total radiated power which passes through the area defined by the 3db beam-width is 47.5%, and the percentage of radiated power within the primary lobe defined by the first nulls is 83.8%.

An array of transmitting elements whose phase shifters are adjusted for a predetermined focal point in the Fresnel zone is termed a "programmed focus" antenna. Its practical size is limited by inhomogeneities of the propagation path over which it operates. When the resulting phase variations are severe enough to invalidate its effectiveness, a self-focusing, or more correctly a "self-phasing" antenna must be used to coherently focus without aberration.

The basic requirements for self-focusing are that a pilot signal be available from the distant terminal, or target point, and that the propagation path be reciprocal. The pilot signal may be a deliberate electronic transmission, a natural radiation from a target object, or back-scattering of an illuminating wave. There is no restriction on the shape of the received wavefront incident at the aperture, nor on the deployment of the subapertures. The subaperture must be small enough so that the propagation medium is nearly homogeneous across it, and large enough to maintain adequate SNR.

1.1.1 Self-focusing Technique

The basic principle of a self-focusing antenna is illustrated in Figure 1. Here the distant terminal is represented as an illuminated target. The key operation is that of phase conjugation, which consists of reversing the signal phase with respect to the reference phase. With this accomplished, it can be shown that the reradiated signal arrives at the target with a phase angle independent of the reciprocal

path length to the subaperture in question. This is the condition required for coherent focusing.

Various methods are available for taking the phase conjugate, including the use of servo-controlled phase shifters. The technique used in the ECI system, and probably the simplest proposed to date, is a double heterodyning operation, illustrated in Figure 2. The required signal phase reversal occurs in Mixer #1, since the local oscillator is higher in frequency than the signal. In Mixer #2 the signal phase is preserved because the upper sideband is the desired output signal. The roles of the two mixers could of course be interchanged by switching their local oscillator sources.

A Linear Focusing Antenna Model (LFAM) was built at ECI for evaluation of the technique under Contract AF30(602)-2297.¹ The experimental program included the design and construction of a 100λ , 25-element model operating at X-band and capable of automatically focusing its transmitted power on an illuminated target in its Fresnel zone. This was followed by an extensive test program to study the Fresnel zone focused fields and self-focusing characteristics. The experimental program accomplished the original objectives but a need was realized for an extension which would permit three-dimensional focusing. The LFAM was converted to a two-dimensional focusing array at the end of the contract.

1.1.2 Benefits of the Two-Dimensional Array

A 2-D focusing array is capable of several interesting experiments which are either impossible or very artificial

-
1. Technical Report on Experimental Program of Steerable Antenna Focusing Investigation (STAFT), Contract No. AF 30(602)-2297: Electronic Communications, Inc., Timonium, Maryland, June 15, 1962.

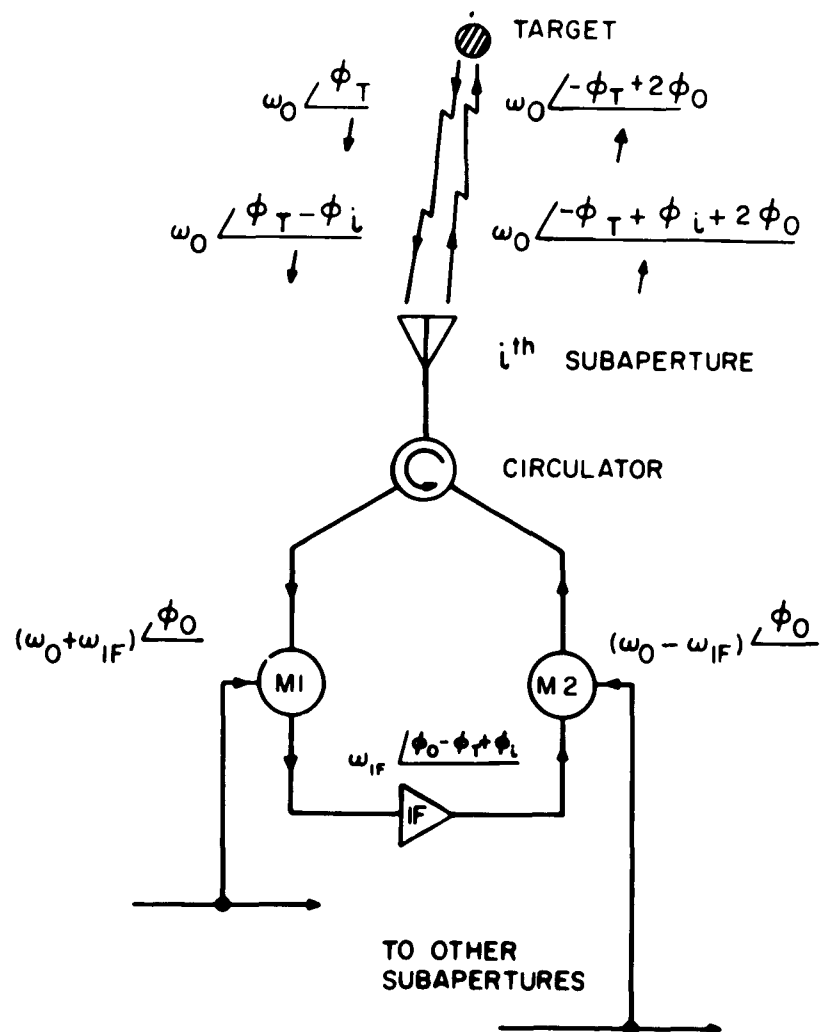


Figure 2. Heterodyne Method for Obtaining the Phase Conjugate

with the LFAM. Reasons for such an extension of the facility include the following.

1) A two-dimensional array provides greater flexibility in element arrangements which resemble a real situation. Suggested arrangements are:

- a) Uniform with high gain horns to fill the aperture to a large extent
- b) Ring(s)
- c) Mills Cross
- d) Linear
- e) Other thinned out distributions

2) Operation of a 2-D array corresponds more closely to expected actual situations.

3) Higher element gain can provide better clutter rejection for operation with unmodulated targets.

4) Realistic power transfer experiments can be performed with a 2-D array.

5) While a central-null pattern can be generated by a linear array, a 2-D array can generate an actual annular ring pattern.

6) Extended, or nonpoint, targets are of interest in anticipated applications. These targets are bounded for any one-dimensional tests. The resulting boundary conditions do not duplicate real targets. No such limitation exists for two-dimensional arrays and tests.

7) A 2-D array with large elements (and as a result, high overall array gain) can concentrate more power on a scatterer for experimental studies of scattering of convergent waves.

2. DESCRIPTION OF TWO-DIMENSIONAL ARRAY

During the final stages of the investigation of the Linear Focusing Antenna Model under Contract AF 30(602)-2297, the array was converted to a two-dimensional configuration. Principally, this consisted of increasing the number of modules to 64 within a framework which would allow maximum flexibility in the disposition of the elements over the aperture area. The electronic modules have been compactly packaged and are permanently mounted behind the array and are connected to their associated antenna element by flexible waveguides. Figure 3 is a photograph showing a rear view of the 2-D array and equipment.

2.1 Specifications

Table I shows the set of specifications which characterizes the array design and construction.

2.2 Construction Features

The design of the 2-D array is presented here in three parts; the receive-transmit subsystem, the reference-signal generating system, and the complete array. In the principle operating mode, energy received by the target from an external illuminating source is modulated with a 200 kc signal. The reradiated signal traverses the path to the array modules where the upper sideband is selected to provide a clutter-free performance.

2.2.1 Module Design

The block diagram of a module is shown in Figure 4. Two sets of antenna elements were designed and built for the 64 element 2-D array. Both designs were adaptations of the conventional pyramidal horn antenna with aperture dimensions of 2λ by 2λ and 6λ by 8λ . The smaller horn offers the maximum flexibility of array element arrangement, yet provides enough gain to operate the 2-D self-focusing array model well above the required signal-to-noise ratios. The horn provides 15.7 db



Figure 3. Rear View of 2-D Array

TABLE 1
2-D Array Specifications

Focusing Method	Conjugate phasing
Operating Modes	Self-focus on modulated or reflector targets, programmed focus
Frequency	X-band, about 9375 Mc
Number of Elements	64
Maximum Array Size	75λ by 75λ (\cong 8 ft by 8 ft)
Maximum Array Dimension	106λ
Antenna Elements	Two provided; 2λ by 2λ , 15.7 db gain, and 6λ by 8λ , 25.3 db gain
Polarization	Linear; either vertical, horizontal, or oblique
Array Configurations Possible	Uniformly spaced square, Ring or concentric rings, Mills Cross, Nonuniform spaced square, Linear
Receiver-Transmit Operation	CW duplexer plus isolation by frequency offset
Receiver Bandwidth	30 kc
Receiver Noise Figure	25 db
Power Output	32 milliwatts
Target Illumination	External 32 db reflector, with 3 watts input
Electronic Scan Capability	At least $\pm 5^\circ$ in azimuth and $+5^\circ$ in elevation
Principle-plane Beamwidth	0.67° in focal plane for square array
Intended Focal Range	10 to 200 feet
Illumination Taper	Up to 35 db variation in element power level

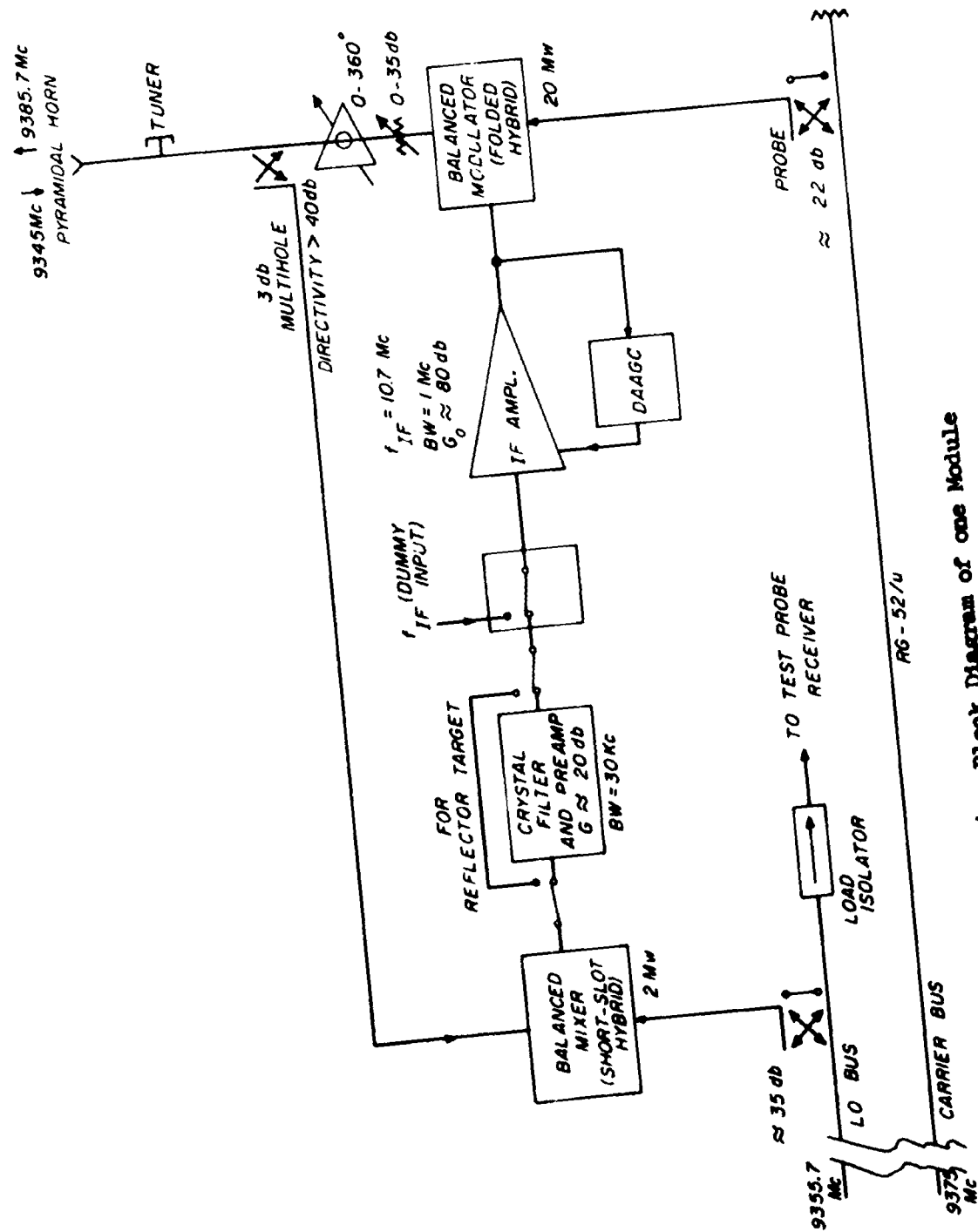


Figure 4. Block Diagram of one Module

of gain with a half-power beamwidth of 23 degrees in the E-plane and 29 degrees in the H-plane. The beamwidths at the -10 db points are 46 degrees and 58 degrees for E and H-planes respectively. The side-lobes occur at 35 degrees from beam center and are 12.3 db down in the E-plane. The radiation patterns for this antenna are shown in Figure 5. The mutual coupling between two adjacent elements with their sides touching is ample enough to maintain good isolation at 35 db when their E-planes are parallel and 37 db when their E-planes are in line.

For some tests of the 2-D array it is advantageous to have additional gain in the antenna elements and, in some instances, a narrower beamwidth than that obtained with the 2λ by 2λ square horn. The grating lobes of the array pattern are reduced by the element factor of a larger horn antenna. The larger antenna also produces a stronger focused field to enhance the measurement of back scattering of a convergent wave and to minimize the effects of clutter return during tests which include a reflector type target. A 6λ by 8λ horn was designed which offers 25.3 db of gain with an E-plane beamwidth of 9 degrees and an H-plane beamwidth of 10 degrees. The -10 db beamwidths are 18 and 20 degrees and the sidelobe level is less than -10 db. The radiation pattern of this horn is shown in Figure 6.

The pyramidal horns receive the "scattered" energy from the target and feed it to the CW duplexer which, in this case, is a 3 db multihole directional coupler. The 3 db transmission and reception losses are tolerable for a demonstration model in trade for the high directivity which is provided by the coupler. The balanced mixer is a conventional short-slot hybrid type fed by 2 milliwatts of local oscillator energy at 9355.7 Mc.

The narrow band 10.7 Mc preamplifier uses a crystal filter for sharp selectivity of the desired target scattered signal. Its

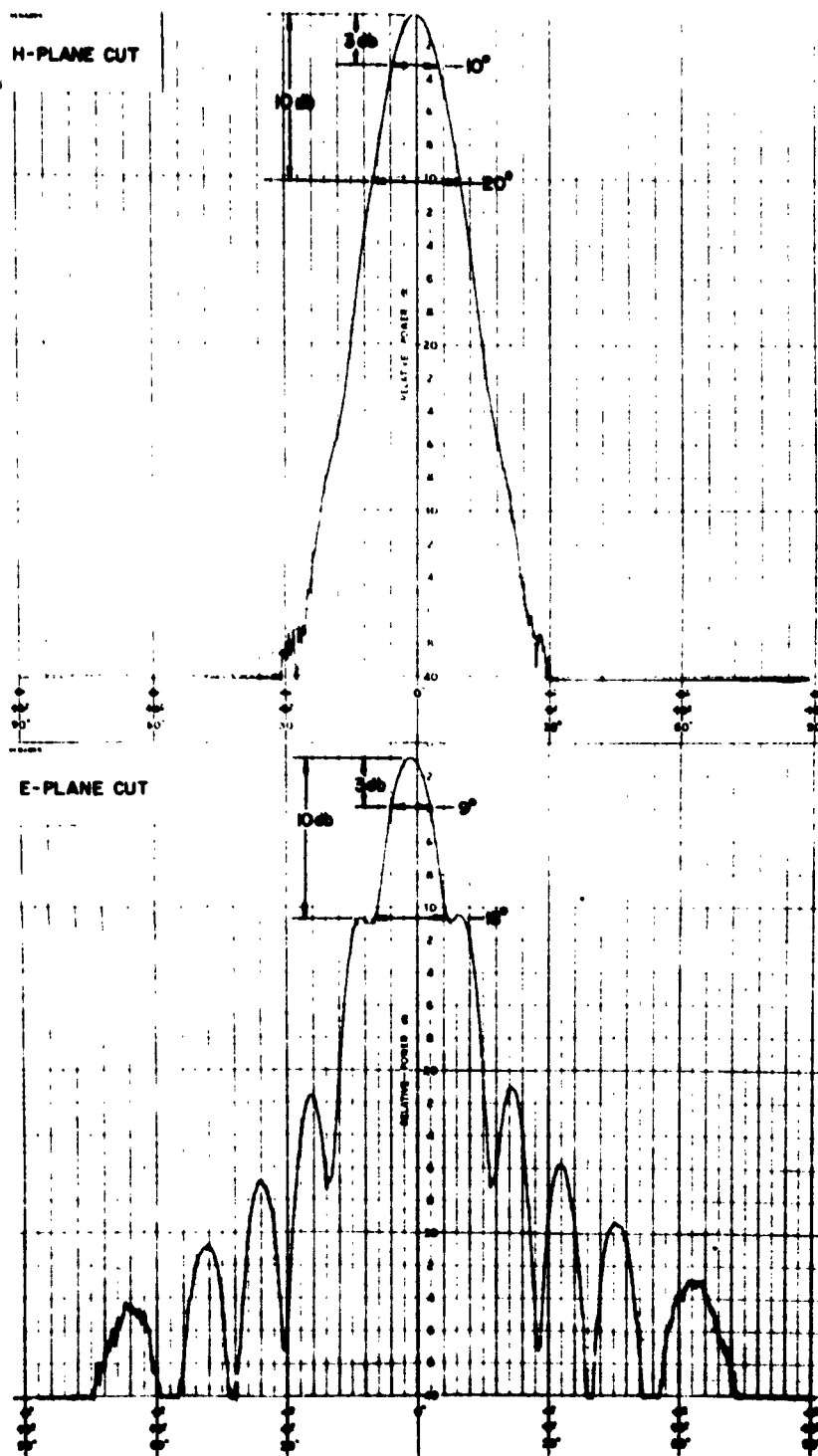


Figure 6. Radiation Pattern of $6\lambda \times 8\lambda$ Horn Antenna

bandwidths at 6 db and 60 db down are 30 kc and 60 kc respectively. This is a critical unit to the phase stability of the system, since the sharp tuning results in a steep phase vs frequency curve. The unit-to-unit reproducibility of crystal filters results in good phase tracking between modules, over the receiver bandwidth. It also results in good phase stability with ambient temperature variation.

In the passive reflector target mode, the preamplifier is bypassed, since its gain is not needed and its selectivity cannot reject clutter. In the programmed focus mode the illuminator and target are not used; a dummy IF signal is fed in parallel to all amplifiers, and the system operates as a phased transmitting array.

The main IF amplifier has a small-signal gain of 80 db and a 1 Mc bandwidth. For the signal level range of interest, the delayed amplified AGC holds the output at an optimum drive for the balanced modulator. The gain control is applied to broadband circuits, so that capacitive detuning is minimized. As a result, the phase change is only 3° for an 80 db range of input level.

The balanced modulator uses a folded magic-tee for compact packaging. It features a carrier suppression of 15 db, a sideband output of about 1 milliwatt, and a conversion efficiency of -10 db. The upper sideband (9385.7 Mc) is used for the focused field; the lower sideband is radiated at the same power level, but is rejected in pattern measurements by the test receiver selectivity.

The modulator output passes through a 0 - 35 db attenuator which is used for amplitude tapering of the aperture illumination, and through a 0 - 360° phase shifter which is used for array adjustment and for programmed focusing. The shifter consists of a short-slot hybrid junction and a waveguide trombone type line stretcher.

The signal finally undergoes a 3 db loss in the duplexer and is radiated at the 0.5 milliwatt level. The antenna tuner serves to minimize reflection from the antenna back through the receiver port of the duplexer. The overall transmitter-receiver isolation is greater than 30 db. This includes the effect of direct duplexer leakage, reflection from antenna mismatch, and mutual coupling from adjacent subapertures. This isolation is of course augmented by the receiver selectivity.

The focused signal is at 9385.7 Mc. This offset in frequency from that received (9345 Mc) results in a slight pointing error whose maximum is a very small fraction of a beamwidth.

The routing of LO and carrier signals to the mixer and modulator inputs of each module is accomplished by means of waveguide buses with individual tap points. In order to maintain phase stability throughout the reference signal complex, the transmission line is entirely made up of waveguide. An adjustable cross guide-probe coupler combination was developed at ECI. Two sections of crossed waveguide are joined at their broad walls, with a 0.200 inch hole cut in the symmetry point of the common wall. The probe goes through a threaded boss, crosses the cross guide, and penetrates an adjustable distance into the main guide. Four waveguide buses having 32 each of the adjustable couplers are used in the 2-D array model. The two buses (one for each module bank) used to distribute carrier power are driven in parallel through a matched shunt tee power divider. Each is provided with a terminating load. The two buses which distribute LO power are connected in series, the remaining power being conducted downrange to serve also as LO to the test probe receiver.

2.2.2 Signal Generation

The signal sources required for the 2-D array model are shown in the block diagram of Figure 7. All microwave signals are

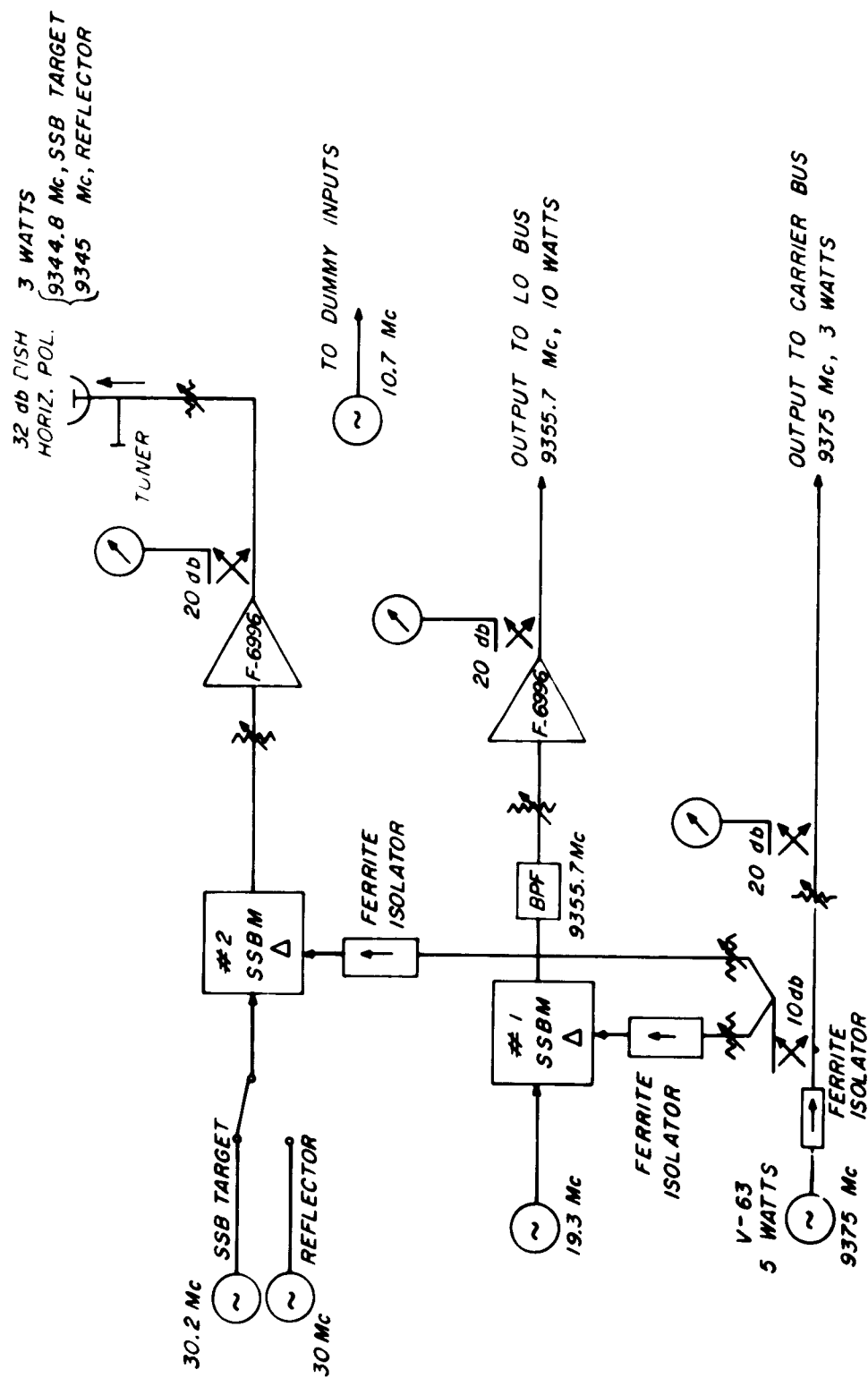


Figure 7. Block Diagram of Signal Generating System

derived from a single RF source, so that the only intersignal frequency drifts are those of crystal oscillators.

A 5 watt klystron oscillator supplies power to the carrier bus and is the source of the transmitted power. A half-power sample from this source serves as the input to two single-sideband modulators which generate the other two RF signals. The isolator absorbs the undesired sideband, which is radiated back from the carrier input port. The bandpass filter eliminates a spurious response. Traveling wave amplifiers of 30 db gain and 10 watt maximum output are used to produce the power required by the local oscillator bus and the illuminator.

The choice of modulating frequency in the upper SSB modulator serves to provide a back-scattered signal at 9345 Mc, regardless of whether the target is a reflector or is modulated at 200 kc.

2.2.3 Complete Array Design

The method devised for module packing in the experimental 2-D array permits extreme flexibility in the deployment of the elements. This consists of spacing the electronic modules associated with the antenna elements rather uniformly on a structure behind the array, mounting the antenna elements wherever desired on a vertical array support structure, and connecting the elements to their electronic modules with flexible, 5-foot, twistable waveguides.

This arrangement of modules was chosen to (1) be reasonably compact, (2) permit convenient adjustment of operating controls, and (3) permit easy removal from the bank for repair or bench test. The LO Input and Carrier Input ports each connect to the waveguide buses. The buses are mounted with their adjustment screws facing right for the LO bus and toward the other bank of modules for the carrier bus. The right hand end of the directional coupler is the

antenna port, to which the 5-foot twistable flexible waveguide connects. A twistable flexible waveguide at the LO Input serves to relieve undue mechanical stress which would arise from the two rigid waveguide buses being connected by many modules having normal dimensional variations.

The electronic modules are mounted in two banks of 32 each. Those in the upper bank are inverted with respect to those in the lower bank, to give ready access to the controls of each from a normal standing position. The modules are mounted on a framework of structural steel which is anchored to the array housing. The spacing of adjacent modules was dictated by the requirement that it be an odd multiple of one-fourth guide wavelength in the waveguide buses. The smallest such multiple which would avoid heavy staggering of the components in adjacent modules was $9/4\lambda_g$, which at 9.375 Gc is 3.96 inches in X-band waveguide. This spacing avoids any component overlap, or staggering, and allows 32 units to fit into the available space.

Mounting of the antenna elements is achieved through use of an adjustable tubular frame. Each horn is clamped by chemistry clamps at the desired height on one of a set of 16 tubular stainless steel columns. Each column is connected through sliding blocks to a pair of heavy horizontal transverse tubular supports. These blocks are clamped to hold a column in the desired position in the array. The two horizontal supports, which carry the entire array, are in turn connected through sliding blocks to four longitudinal tubular supports anchored to the floor and ceiling of the array housing. The sliding blocks enable the structure to accommodate either of two sets of horns with greatly different lengths, while supporting them near the apex.

2.3 Field Measurement System

The procedures used for measuring transverse and axial patterns of the LFAM (reference 1) are not suitable for the tests and

measurements to be performed with the 2-dimensional array model. Adding another dimension to the array and to its focusing capability creates new problems in pattern measurement. Those necessitating the design of new techniques and equipment are discussed below with the design solutions.

2.3.1 Probe Tower Design

In the LFAM program, the vertical beamwidth of the array was that of the elements, or 5 degrees. At the typical ranges of 20 to 200 feet, the vertical spot size was then 21 to 210 inches. The corresponding errors in vertical position for 0.5 db directivity loss were, respectively, 9 inches and 90 inches. The test roadbed is flat within 2 or 3 inches across its 20 foot width, and has a 21 inch bow in its 200 foot length. The combination of the vertical tolerances and the dimensional characteristics of the test roadbed allowed the use of a constant height test probe carriage, rolling on the test roadway, without introducing significant boresight errors into the measurements. Azimuth control of the test probe position was facilitated by calibration lines painted on the roadbed.

In extending the array to two dimensions, the reduction of vertical beamwidth from 5 to 0.7 degrees, a factor of 7 to 1 meant that the position tolerance at short ranges would be little more than one inch in elevation and azimuth. This degree of control must also be maintained in taking axial patterns. The difficulty is compounded by the requirement for taking vertical, horizontal, and oblique patterns in the focal plane, through focal points which vary in elevation and azimuth.

A further point of the test probe position control problem arises from the required height of vertical probing. This has been determined to be about 20 feet above the metallic base structure of the probe tower. If a mobile tower of several feet wheelbase is rolled on

the test roadway, as in the LFAM program, small rises and depressions in the roadway would appear as magnified horizontal motions at the top of the tower. This difficulty is avoided with the rails and carriages described above. Also, the rigidity of the carriages and of the large mast minimize vibration and wind effects on the test probe position.

It was determined that no ready solution could be derived from the original method of rolling the test probe carriage on the test roadway. Instead, a pair of rails has been provided, straddling the present roadbed, to give a constant slope of 3° to a distance of 137 feet. The rails and their supports are of wood to minimize interference with the radiation fields. They are straight, parallel, and of equal elevation, to within less than a quarter of an inch.

The rails support a rolling field probing carriage system, which spans the roadway as shown in Figure 8. The lower carriage (called the 'rail carriage') is fabricated of aluminum structural sections, and rolls on the wooden rails for recording axial patterns or for fixing the range for transverse pattern taking. A smaller carriage (called the "mast carriage") rolls horizontally on the rails of the rail carriage, moving in a horizontal transverse direction. This motion serves to scan the test probe for horizontal transverse pattern recording, and also to fix the azimuth position for vertical transverse patterns. A 20 foot vertical fiberglass mast is mounted on the mast carriage. The test probe antenna and RF head are carried along this mast by a small carriage called the "probe carriage". This motion serves to scan the test probe for vertical transverse pattern recording, and also to fix the vertical position for horizontal transverse or axial patterns. Simultaneous movement in both the horizontal and vertical directions causes the probe to follow an oblique angle path in the transverse plane for measurement of beam circularity.

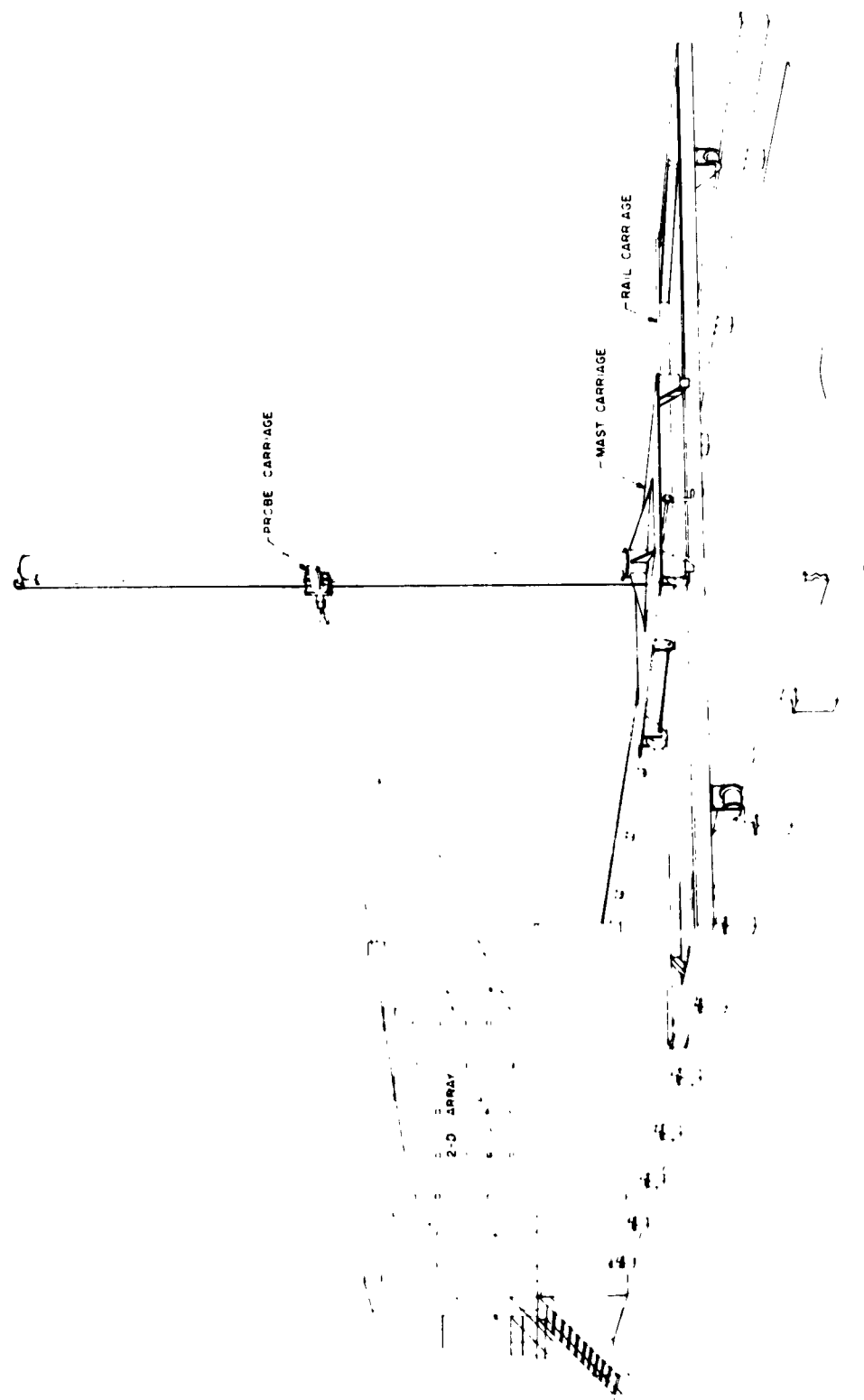


Figure 8. Test Probe Assembly

The use of rail directed scanning in rectangular coordinates is expected to limit errors in position of the test probe antenna to about one inch.

The design of the probing system is complete and the construction has reached a 60% state of completion. The rail system was the first part of the equipment to be installed. Six-foot, six inch by six inch treated posts were precisely located every twelve feet along the roadbed and placed in concrete to a depth of three feet. The tops of the posts were cut along a transit-sighted line three degrees from horizontal. Angles with enlarged mounting holes to facilitate critical adjustments were affixed to the tops of the posts. Two inch by six inch, air-dried oak beams were attached to the angles for a distance of 137 feet from the array.

The rail carriage consists of a rectangular reenforced framework five feet deep by twenty-five feet wide made up principally of five-inch aluminum I-beams. The wheels attached to the I-beam structure are flanged to maintain alignment and tracking on the oak rails. Axial radiation patterns are made by pushing the rail carriage toward the array from down range. The I-beams act as the rails which carry the mast carriage in the horizontal movement. Maximum deflection of the I-beams with the entire load at the center has been calculated to be less than 0.5 inch. Azimuth positions of the mast from ten feet on either side of array boresight can be achieved. All parts of the mobile probe equipment which are, of necessity, made up of metal are confined to within an area which is 30 inches above the roadbed. In this way the interference due to path reflections can be easily controlled and, most likely, entirely eliminated.

The mast carriage consists of a five-foot by five-foot platform on gear-driven wheels which ride the I-beams of the rail carriage. The gear-train assembly can be disengaged and shifted to provide vertical

movement of the probe without horizontal movement, or horizontal movement of the probe without vertical movement, or both movements simultaneously for a 45° oblique angle. A hand crank at the rear of the carriage assembly is the only drive point for the entire operation. The mast carriage is moved by means of a chain drive to the gear assembly which is driven by the hand crank. Vertical movement of the probe up and down the mast is achieved by a nylon-rope and pulley arrangement which is also driven by the gear train assembly. From the base of the mast upwards, all parts are non-metallic. The mast is a 20-foot fiber-glass laminate tube with an outside diameter of $4 \frac{7}{8}$ inches. A phenolic track is mounted on one side of the mast. A four-wheeled carriage to which the test probe receiver is clamped rides on the phenolic track over most of the mast height enabling a total vertical probe positioning from 10 feet above to six feet below the array boresight.

The test probe receiver will be the same as that used in the LFAM experiment. The pyramidal horn will feed the probed signal through a tunable cavity filter which preselects the 9385.7 Mc to the mixer. Local oscillator energy is removed from the waveguide bus in the underground conduit at the side of the roadbed and brought to the mixer by means of a short run of coaxial cable. The 30 Mc IF signal is fed back to the array housing through the video cable in the conduit to the X-Y recorder. X and Y position information signals are wire fed to the recorder from 10-turn helipots attached to both the horizontal and the vertical drives.

2.3.2 Reflection Baffles

Reflections, or multipath signals, are a common problem in overland pattern ranges. In the LFAM program this problem did not arise because of the high vertical directivity of the hoghorn elements used. The $2\lambda \times 2\lambda$ elements ordinarily used in the 2-D array do little to attenuate reflections.

Signals arriving at the test probe receiver over indirect paths were examined during a test site evaluation. It was found that roadbed reflections could be reduced greatly with vertical baffles of microwave absorbing material placed about midway between the array and the focal point, and extendable to a height of six feet. The required height varies depending upon the focal distance, but cannot exceed six feet. At focal ranges of 100 feet or more a second baffle of less height is required somewhere between the first baffle and the focal point. Two such baffle structures are being provided, each sixteen feet wide, with maximum heights of six and four feet, which are readily rolled to the required positions. The baffles are foldable for quick storage beneath the test probe carriage assembly in an enclosure which has been specifically designed and built for this purpose. All field measurement equipment, with the exception of the target-support tower, is housed in the enclosure located on the roadbed at the foot of the array or in a compartment at the side of the array housing. In this way quick set-up time and dismantling time has been provided as an adjunct to the rapid measurements anticipated through use of the probe system already described.

2.4 Illumination Monitor

2.4.1 Description

In a large steerable array antenna which is operational in its purpose, occasional failures and misadjustments of individual elements can usually be tolerated, so long as they are statistically few. However, a research model demands more careful control, since one is ordinarily attempting to determine what is the best possible level of performance. In the LFAM the phase and amplitude of the aperture illumination function are adjusted by comparing each element output to that of a reference element. The comparison is made in the test probe receiver at

a distant field point, by a nulling technique. The procedure is described in detail in Reference 1. The point here is that each element must be turned on individually, adjusted, turned off, then the next element, and so forth. In order to check the array adjustment one must repeat the entire adjusting procedure.

With the number of elements increased from 25 to 64, it became apparent that a more direct and convenient method was needed, both for initial adjustments and for occasional checks on the adjustment. Accordingly, an instrument called an "Aperture Illumination Monitor" was devised which presents an oscilloscopic display of the relative transmitted phases and amplitudes of all the elements. The signals are not actually measured at the aperture, but instead are picked up at the focal point by the test probe receiver, at a distance such that all elements are effectively boresighted at that point. A description of the Illumination Monitor is given below.

A block diagram of the Illumination Monitor for measuring the relative amplitudes and relative phases transmitted by all array modules is given in Figure 9. Initially, all of the modules are turned "off" by a bias applied to the last two stages of each 10.7 Mc amplifier, providing an attenuation of greater than 70 db, which is sufficient for this application. A 64 position motor driven selector switch* sequentially removes the bias from each IF amplifier, turning "on" the module associated with that IF amplifier. The selector switch has an "on-off" duty of 50% and a rotational speed of 20 rps; thus each module is gated "on" for approximately 0.39 msec every 50 msec.

During the module "on" time a signal from the target horn is received and retransmitted by that module. The retransmitted

* This switch is of the jet mercury commutator type called a Delta-Switch, made by Advanced Technology Laboratories.

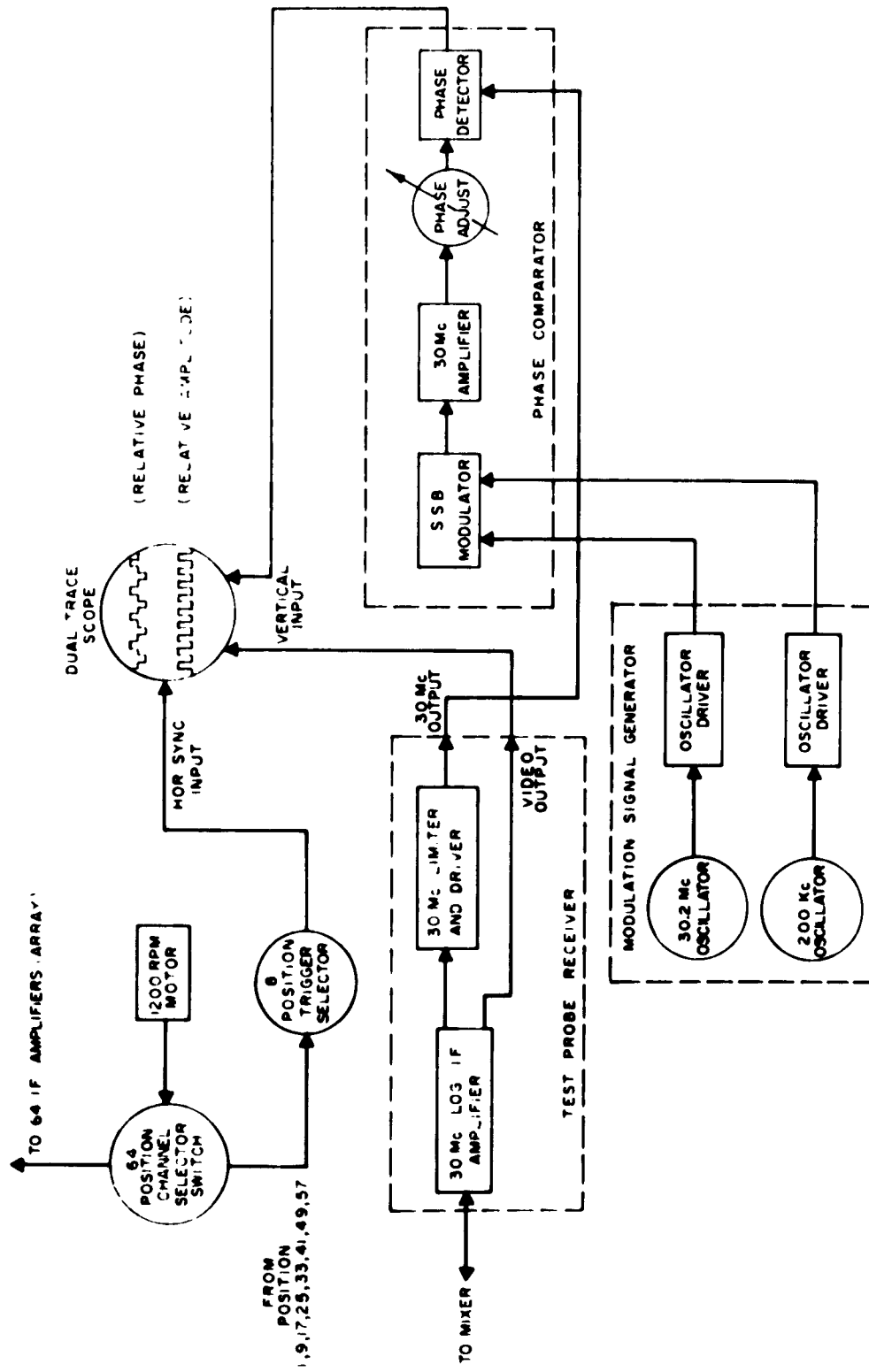


Figure 9. Block Diagram of Illumination Monitor

module signal is then received by the Test Probe (pattern recording) Receiver, which is described in Reference 1. The log IF amplifier in the Test Probe Receiver has been modified to provide a 30 Mc output for phase monitoring; also the video bandwidth has been increased to follow the 0.39 msec gating pulse waveform. The gated log IF video signal is used as one vertical input of a dual trace scope to display the relative amplitudes of each module. To generate the horizontal sweep, an external trigger pulse is derived from the 64 position selector switch to trigger the internal scope sweep. Therefore, to display the relative amplitudes of the 64 modules on a single display, the horizontal sweep time is adjusted to 50 msec and triggered by a pulse from Position 1. Because of the difficulty of visually counting to the i^{th} module an expanded scale is provided, by increasing the sweep rate by a factor of 8 to 6.25 msec, thus displaying only 8 module outputs. Then, by selecting the proper horizontal trigger, any one of 8 groups each containing 8 module output signals can be displayed. A photograph of the relative amplitude display of 8 modules is shown in Figure 10.

A relative phase measurement of each module output is also made during the 0.39 msec module "on" time. A 30 Mc phase reference is obtained by mixing the 30.2 Mc and 200 kc array oscillators in a single-sideband modulator. The 30 Mc reference is then used as one input to a phase detector, and the (coherent) 30 Mc log IF output as the other. The phase detector output characteristic has the typical "S" curve shape whose phase range is $\pm \pi/2$ radians. The procedure for phasing the array is to observe (on the scope display) the phase difference between each module and the reference, then vary the phase shifter of the corresponding module until the difference is nulled. Figure 10 (a) and (b) shows 8 modules with relative phase and amplitude out of adjustment, and in adjustment respectively. By observing Figure 10 (b) after phasing,

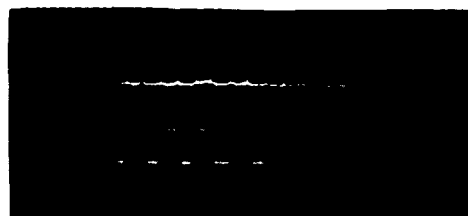
(a)



(RELATIVE PHASE)

(RELATIVE AMPLITUDE)

(b)



(RELATIVE PHASE)

(RELATIVE AMPLITUDE)

Figure 10. Illumination Function Display

"spikes" are seen at the leading and trailing edges of each pulse. These spikes are caused by the phase modulation of the received signal as the module is turned "on" and "off". If the modules are 180° out of phase, as are the 2nd and 3rd modules (counting from the left) in Figure 10 (a), the spikes will appear reversed. Therefore, to remove this phasing ambiguity these spikes were purposely preserved in the circuit design and used as part of the display.

2.4.2 Effect of Motion Caused by Wind Gusts

Mechanical motion caused by wind gusts at the illuminator antenna, target horn, and test probe horn cause fluctuations of the phase measurements displayed on the monitor. Since the motion is much slower than the monitor sampling rate, the same phase change is observed at all elements. Presently this shift is compensated by a manual adjustment which is adequate but tends to make the array alignment somewhat difficult. To overcome this difficulty an automatic circuit is being designed to compensate for the undesired phased delay. Briefly, this circuit operates on the phase-reference oscillator so that the phase reference includes the changes introduced by wind gusts. This modification will be tested and fully described in the next quarterly report.

3. TEST PROGRAM

A preliminary study of the tests is to be performed on the two-dimensional array model. The test procedures which describe each task in detail will be submitted before the test begins. The procedures for the first Test Group which involves the collection of Fresnel zone radiation pattern data for the square aperture array in programmed and self-focusing modes, for a point focus has been prepared. The details for the conical radiation pattern tests (Test Group 2) are presently under consideration. A discussion of the scattering problem as it relates to a spherically converging wave is included in the Appendix.

3.1 Outline of Tests

The tests to be conducted with the two-dimensional array include the following:

3.1.1 Fresnel zone Radiation Patterns of a Square Aperture

The proper evaluation of planar self-focusing arrays requires basic pattern data. Such data is essential to all potential applications of the self-focusing technique. Therefore a systematic experimental study will first be made of the radiated field distributions from the 2-D array with rectangular element configuration and equal spacing. The patterns are to be taken primarily in the self-focusing mode, with a point focus, although a set of program-focused patterns will be included.

Transverse patterns will be taken for horizontal vertical, and oblique directions at several ranges in and around the focal plane. This will include measurements at central and extreme values of target range and azimuth. These measurements will be made using the small ($2\lambda \times 2\lambda$) elements in the array. They will be

repeated using the large (about $8\lambda \times 6\lambda$) elements, insofar as is necessary to evaluate the effect of element factor on overall performance. The initial patterns will be evaluated to determine limitations imposed on pattern accuracy by such factors as adjustment imperfections, thermal drift, mutual coupling between elements, element factor, test range multipath, clutter, and illuminator-to-array leakage. In addition, errors in recording the true patterns, which might be caused by test probe travel errors, test probe antenna directivity, position detecting errors, or wind motion of the test probe will be determined.

Axial patterns will be taken for several target ranges and azimuths along the beam boresight of the array using the small horn elements. The data obtained from the transverse and axial tests above will provide tests of range and azimuth tracking in addition. These will be carefully studied for any anomolous behavior. No inherent tracking errors were detected when testing the linear array; however, the axial field pattern is much more sharply focused in the 2-D array, and of course a better model of typical applications.

Tests will be made with the array in the programmed focus mode of operation to compare selected critical patterns with those taken in the self-focusing mode. The time and temperature stability of the system is particularly significant in this mode of operation.

In the LFAM program, the vertical beam was sufficiently broad that the test probe could be offset from the target in elevation angle without appreciable drop in field strength. At ranges equal to or less than the target range the test probe was lower

than the target; at greater ranges it was higher than the target so that no blocking of any rays resulted.

However, a blocking problem arises in the present program from focusing in the vertical dimension as well. One possible solution is to reduce the field probing equipment to the point that its shadowing effect is insignificant; in practice this is not feasible. A more attractive method is to offset the focal spot from the target in both azimuth and elevation. This is accomplished by offsetting the test probe from the target when the array is initially adjusted, or "phased out." The offset is in effect a deliberate angle pointing error. The value is chosen such that the target occupies a position of minimum interest in pattern recording. As an example, at a range of 500λ (52.5 feet), the target could be one foot above and one foot left of the focal point. Then with a focal spot width of 0.65 feet for a $75\lambda \times 75\lambda$ aperture, vertical and horizontal transverse patterns could be taken in the focal plane without interference. Also, an oblique transverse cut, running from lower left to upper right, could be taken to determine beam circularity. At this point the focusing array system will contain deliberate angle tracking errors of about 1.1 degrees in both azimuth and elevation. If range tracking tests are to be performed, this must be taken into account. Thus if the target is moved to 1000λ range, it should be positioned two feet above and 2 feet left of the expected focal point.

At ranges other than the focal range, a further blocking or shadowing problem exists. This is depicted in one plane by Figure 11, where the shadow regions are shown shaded. At short ranges, the array is partially blocked by the test probe from receiving the scattered illumination from the target; at long ranges the test

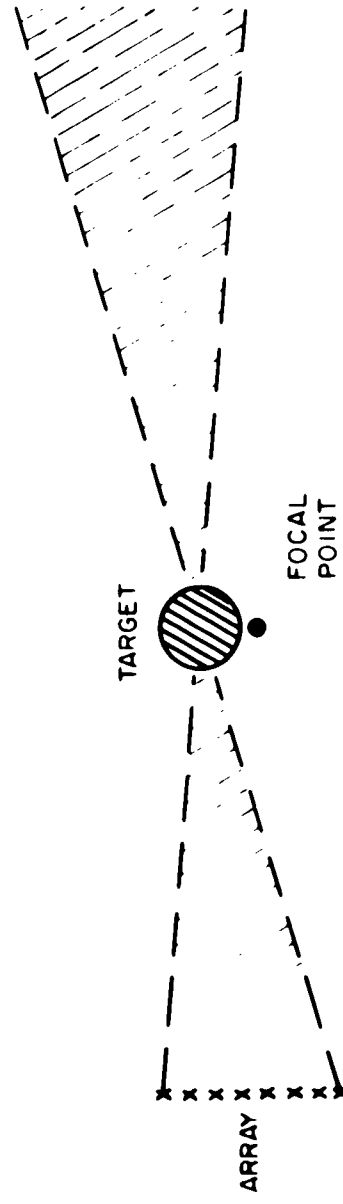


Figure 11. Shadow Regions in 2-D Array Testing

probe is partially blocked by the target from receiving the array transmitted signal. The extent of the shadowed region increases with distance from the focal plane. The treatment of this problem varies with three different situations.

Where tracking tests are being conducted, only the focal region is of interest, so that the blocking problem of Figure 11 can be ignored. When the field outside the focal plane must be recorded, in some cases the target can be offset a considerable distance from the focal point, so that the shadow regions do not overlap any of the region for recording. The latter technique will not be suitable when patterns must be recorded at ranges very short compared to the focal range, nor when patterns must be taken over broad angles from the array axis. Also, the allowable offset is limited by the directivity of the elements in the array, particularly when the large ($6\lambda \times 8\lambda$) horns are used. In these latter cases where target offset is not an adequate solution, it is necessary to record the patterns in the programmed focus mode of array operation. In this mode there are no blocking problems.

3.1.2 Conical Radiation Pattern Study

In certain applications it is desired to generate a radiation pattern with a null in the direction of the antenna axis. The radiation pattern would thus be conical or annular in shape. Previously, we have investigated analytically the type of aperture distributions required to achieve such radiation patterns. The general characteristic of the aperture distribution that gives rise to the null on axis is that the phase distribution across the aperture, after subtracting the phase distribution required for focusing, must integrate to zero. It is proposed to experimentally investigate the radiation patterns of the two-dimensional self-focusing antenna designed to

produce a conical pattern with a null in the direction of the target. Tests will be conducted to determine: (1) how well the experimental patterns match the theoretical predictions, and (2) the depth of the null in the direction of the target. Particular attention will be paid to the radiation pattern in planes other than that through the focus since the performance of the intended application will be affected by the radiation in the vicinity of the focal plane as well as the energy passing through the focal plane.

These tests will be conducted with a point target, in either the self-focus or programmed focus mode of operations. Since another task in this test program may include a determination of the effect of an extended target on the conical pattern, self-focusing will probably be the chosen mode. A final choice will result from a study presently underway of the detailed techniques needed to instrument the two possible modes for conical patterns.

The conical radiation pattern will be studied using a multiple ring arrangement of the elements in the array. The square array arrangement will also be tested if a suitable phase distribution can be devised.

3.1.3 Extended Target Study

The self-focusing technique was developed theoretically for a single point target, and has been extended to apply to multiple point targets. However, the behavior of a self-focusing antenna with a continuous target whose dimensions are greater than the spot size is not established. A suitable extended passive reflector target will be designed and constructed to test the self-focused patterns in the focal region. The resulting patterns will be compared to the

reflectance (or brightness) distribution of the target configuration. An additional interesting evaluation is a comparison of the power intercepted by the target to that which is intercepted from a programmed focus beam directed at the target center. This comparison can be made by integrating the field patterns over the target extent, for the two modes of operation.

These tests will be conducted using the square array arrangement. The simplest extended target configurations are planar and curved metal surfaces, where typical dimensions are about 10 feet. A more versatile arrangement can be provided by mounting small elementary reflectors in mosaic fashion on a supporting sheet of absorbing material. In this manner the local brightness can be varied in a predictable manner by control of the areal density of the small reflectors.

3.1.4 Scattering in Convergent Fields

The availability of convergent fields presents a unique opportunity for studying scattering phenomena. The characteristics of targets for image formation, power transfer, and for reference purposes, may be investigated with the 2-D array. The results obtained are expected to be of considerable value in these areas. Additional discussion of this study is presented in the Appendix.

3.1.5 Other Aperture Arrangements

In addition to the uniformly spaced rectangular arrangement, the following configurations will be investigated in the manner described in paragraphs 3.1.1, 3.1.2, and 3.1.3.

- 1) various non-uniform spacings in a rectangular array
- 2) single and/or multiple rings
- 3) crossed linear arrays.

The extent of the work in each case will be determined by the significance of the results obtained. In some cases, agreement with previous results is expected to permit a limited schedule of measurements. This will allow a more extensive effort on the remaining arrangements.

3.2 Program For Next Period

During the next quarter, the field probing system will be put into operation. The initial tests will determine the limitations imposed on the system accuracy by such factors as adjustment imperfections, instabilities, test site characteristics, clutter, and test probe travel errors. The transverse and axial patterns as discussed in Section 3.1.1 will be measured. The test procedures for Group No. 2 tests, Conical Radiation Pattern Study, and for Group No. 3 tests, Extended Target Study, will be prepared and submitted for approval. The tests of conical radiation patterns will be completed during the last part of the period and preparation of the scattering in a convergent wave field test procedure will be started.

4. APPENDIX - SCATTERING OF CONVERGENT WAVES

1. Introduction

Scattering of electromagnetic radiation has been a time honored study since even before the early work of Lord Rayleigh. Typically, the incident radiation is linearly polarized, plane wave. There appears to be very little experimental or analytical work using non-planar waves. Experimental studies heretofore have lacked the mechanism to perform such a study conveniently. Because large antennas which "focus" on targets create a partial spherically converging wave, it is important to investigate the scattering properties of objects in a non-planar wave environment. This discussion will outline the initial problem and propose the type of experiment that may be conducted.

1.1 Definition of Terms

The definition of scattering terms appears in different forms as used by various authors. The definitions as outlined by King and Wu¹ will be utilized. If the incident field as generated by a source is denoted by \underline{E}^i and \underline{H}^i which in turn are incident on a passive object on which currents are set up, then a scattered, reflected, or reradiated field exists and is defined to be the scattered field. This field will be represented by \underline{E}^s and \underline{H}^s following the superscript notation. The total field \underline{E} , \underline{H} is the vector sum of the incident and scattered fields. That is, $\underline{E} = \underline{E}^i + \underline{E}^s$, $\underline{H} = \underline{H}^i + \underline{H}^s$. For each field an associated Poynting vector may be defined in the form $\underline{S} = \underline{E} \times \underline{H}$.

It is possible to define certain average quantities to characterize the reradiating properties of an obstacle in an incident plane wave (p-wave) field. These quantities should still be meaningful

1. R.W.P. King and T.T. Wu, "The Scattering and Diffraction of Waves," Harvard University Press, Cambridge, Mass., 1959.

if the incident field is converging. Let S^i be the scalar magnitude of the real part of the incident complex Poynting vector \underline{S}^i at the location of the obstacle. Let P^s be the total scattered or reradiated power. If the discussion is confined to perfectly conducting, non-absorbing obstacles, then P^s is equal to S^i . The total back-scattering cross-section is

$$\sigma = \frac{P_{\text{isotropic}}^s}{S^i}, \text{ where } P_{\text{isotropic}}^s \text{ is the total power}$$

radiated by a fictitious isotropic source. In radar the monostatic case is usually considered, but it is proposed to also include bistatic scattering in the STAFT studies. It appears, however, that the initial efforts will be made only in the back-scattering region.

The back-scattering region will be investigated because it is only in this region that the scattered field can be measured independent of the incident field without additional circuitry. Of course, the incident field can be measured with and without the scattering obstacle and differences taken to determine the scattering field. But King and Wu¹ point out that in general, the incident field is not independent of the scattered field in the sense that the currents and charges in the source are not the same when the obstacle is present as when it is removed to infinity. However, in theoretical problems, it is usually assumed that the source is so loosely coupled to the obstacle that the currents and charges in the source may be regarded as independent of those in the obstacle. Thus, a large separation should be maintained between the source and the scattering obstacle.

1.2 Parameters to Be Measured.

The mean intensity of the energy flow in a harmonic electromagnetic field is $\bar{S} = 1/2 \operatorname{Re} (\underline{E} \times \underline{H}^*)$, and it is this parameter

that is measured by the probe in the scattering field. The requirements of the probe will be discussed later.

The intensity, however, is only one quantity used to describe the scattered field although it is probably the most important. Phase and polarization measurements are also required. Typically, the phase and polarization are expressed for scattering objects in terms of four complex numbers, but it appears that the actual determination of these numbers will be beyond the scope of this experiment.

A reasonable initial investigation would include a measurement of intensity which allowed easy comparison of the monostatic cross-section due to plane wave (p-wave) incidence and spherically converging wave (sc-wave) incidence. The technique for such a measurement will be discussed later. Polarization due to scattering can be measured in terms of the E_0 , and E_ϕ components of the intensity, and phase measurements should probably be postponed.

2. The Forms of Scattering

Before discussing actual experimental requirements, it is wise to consider that scattering analyses are usually divided into three principal regions according to the ratio of wavelength to obstacle size. These principal forms are classified as follows:

- 1) Wavelength large compared with obstacle dimensions - Rayleigh scattering.
- 2) Wavelength of the same order as obstacle dimensions - "Resonance" region.
- 3) Wavelength small compared with obstacle dimensions - "Physical Optics" region.

Rayleigh scattering occurs for objects small compared with the wavelength so that in this region fine details of the target do not affect the scattering cross-section. For p-waves incident on various

objects, the cross-section is usually proportional to a^6/λ^4 , a being a measure of the dimensions of the object. It is believed that the Rayleigh scattering cross-section will not be significantly changed if a sc-wave is used instead of a p-wave. Electromagnetic radiation cannot be "focused" into a region having dimensions which are less than a wavelength. If the scatterer is considerably smaller than a wavelength, then the object probably will not "recognize" any of the phase characteristics of the incident wave, and will be sensitive primarily to the intensity. There may well be a much larger signal scattered from such an object in a sc-wave than from a p-wave due to increased incident intensity of the focused source. However, the cross-section should remain essentially unchanged, since it is a ratio of scattered intensity to incident intensity.

The physical optics region is the opposite extreme to the Rayleigh region. Here the object is much greater in size than the wavelength and the scattered field can be determined using the scalar wave equation or the Huygen-Kirchhoff expression for the field. The approximation improves as the scatterer dimensions increase. For a very large sphere with a concentric sc-wave incident, the scatterer should reflect a spherically diverging wave that would appear to originate from an isotropic source located at the sphere center. This would be modified if the incident wave were only a portion of a complete sc-wave, and the degree of modification is not known at this point.

Scattering in the resonance region should prove to be the most interesting and the most difficult. Primary effort should be exerted in this area, but not at the exclusion of the two peripheral regions. The approach should include both a theoretical analysis and experimental verification.

A preliminary review of the literature indicates that there have been no scattering studies performed for non-planar wave incidence, either analytical or experimental. This implies that

- 1) the problem is too simple to justify publication, or
- 2) there has been no interest in such a problem, or
- 3) no solution has been found.

An initial look at the problem does not indicate that its solution is easy, especially if only a segment of a sc-wave is discussed. Lack of interest has probably been dictated due to lack of experimental facilities. It seems then that the latter two reasons probably are responsible for no work appearing in the literature. The problem should be studied analytically – at least to the extent of understanding just how large an effort would be required to obtain a solution. Such analyses would concentrate only on the resonance region, because conventional analysis can be modified to obtain approximate solutions in the other regions.

3. Source

The source is an important tool in a scattering experiment. For this study the planar array designed for STAFT will be utilized to generate both planar and converging (spherical) waves. It should be indicated at the outset that the STAFT array can at best only approximate a sc-wave. First, consider the 8 x 8 element array. The phase across any one element is constant so that the spherically converging wave is approximated discretely. Second, the separation between elements (if they are separated) creates unfilled "holes" in the converging radiation field which ideally should contain energy in the proper phase as though it came from a continuous aperture.

It is then appropriate to establish initially the lines of constant contours in the converging beam. Ideally, they should be

spherical. The deviation from a true spherical wave will ultimately establish the size of the largest scatterer to be investigated. Some criterion must be established for this deviation, but it would seem reasonable to allow $\pi/8$ radians phase deviation.

The choice of elements for the array is limited to $2\lambda \times 2\lambda$ or $6\lambda \times 8\lambda$. Because of the need of approximating the continuous aperture it is recommended that the larger elements be used. Hence, the minimum size array using all elements in an 8×8 configuration would be $64\lambda \times 48\lambda$ or $56\lambda \times 54\lambda$ in a 7×9 grid. In some instances the more square rectangular configuration might be preferred.

Another feature is that even with a perfectly spherical wave radiated from the source, it is limited to a solid angle which is proportional to the ratio of

$$\frac{\text{Area of the Array}}{\text{Square of the Distance from Array to Point of Beam Convergence}}$$

The requirements for the solid angle are to be explored further, but the upper and lower bounds are established by other restraints. The minimum displacement between the source and scattering obstacle is determined by the size of the individual elements in the source, since it is usually much larger than the scatterer. The maximum displacement is set by the size of the full array, as there is a limit to the distance over which it can effectively focus. Unless the array is operated with a limited number of elements or with the smaller elements, its size is essentially fixed between 55λ and 75λ on a side.

4. The Scatterers

Since there are three regions to be investigated, it appears that more than one source for scattering will be required (the frequency of the array is essentially fixed). Thus, there will be a number of objects made identically, except for their dimensions. Traditionally,

the sphere has been used because the problem has been solved for p-wave incidence and it can be modeled conveniently. The sphere is used as a scattering standard. If sc-waves are used the sphere is an even more logical first choice, since its boundary can be made to coincide with the converging wave front by placing the sphere center concentric to the focus of the sc-wave. Thus, it is recommended that the sphere be studied exclusively.

The size of the sphere determines the region in which scattering is being conducted, i.e., the physical optics region. As indicated previously, primary effort should be in the resonance region, but the other two regions should be investigated.

In the Rayleigh region a plot of σ versus λ on logarithmic paper for a p-wave incident on a sphere is a straight line of slope -4, due to the a^6/λ^4 dependence of σ . Two different size spheres would be minimal to verify such a slope for sc-wave scattering. The largest sphere that can be said to give Rayleigh scattering is $a \approx \frac{\lambda}{10}$. The smallest sphere size is determined on the basis of the sensitivity of the measuring system.

At the other extreme region the largest sphere size is determined by the phase contours that must be experimentally measured. In order that the sphere dimensions be in the physical optics region, the radius must be at least 10λ . However, it is believed that one sphere on the order of this size will suffice.

The number of needed sphere sizes in the resonance region is open for discussion. For this type of scattering σ plotted as a function of wavelength is highly oscillatory, at least for p-wave incidence. There is no reason at this time to expect scattering in this region to be non-oscillatory because of sc-wave incidence. An analytical input at this point would be most useful because the sphere sizes could be

chosen to verify the predicted cross-section at critical points. However, lacking such data it seems reasonable (on the basis of p-wave scattering) to use spheres having radii of 0.5λ , 1.0λ , 3.0λ . This is definitely a minimal number. To investigate the resonance region properly, at least six more spheres are needed with dimensions between 0.5λ and 1.0λ . It appears then that 9 or 10 spheres would be adequate for the resonance region. Hence, to explore fully sc-wave scattering approximately a dozen spheres will be needed as scattering sources.

5. Conclusions

This scattering discussion has sought to review the scattering problem in an intuitive way and indicate the nature of an experimental program. It may serve as an initial guide for the experiment and to provoke thought for further work. The entire problem has thus far been an academic one with little application to any specific problem. Such work should be studied in detail for the backscatter region, because these patterns are the same as those from a wide baseline antenna "focused" on an earth satellite. Other unique characteristics may exist for a partial sc-wave on a scattering object, especially if it could be examined in two scattering regions (i.e., two greatly different frequencies).